

Organics in comet 67P – a first comparative analysis of mass spectra from ROSINA–DFMS, COSAC and Ptolemy

Kathrin Altwegg, Hans Balsiger, Jean-Jacques Berthelier, André Bieler, Ursina Calmonte, Stephen A. Fuselier, Fred Goesmann, Sébastien Gasc, Tamas I. Gombosi, Léna Le Roy, et al.

▶ **To cite this version:**

Kathrin Altwegg, Hans Balsiger, Jean-Jacques Berthelier, André Bieler, Ursina Calmonte, et al.. Organics in comet 67P – a first comparative analysis of mass spectra from ROSINA–DFMS, COSAC and Ptolemy. Monthly Notices of the Royal Astronomical Society, 2017, 469 (Suppl_2), pp.S130 - S141. 10.1093/mnras/stx1415 . insu-01574263

HAL Id: insu-01574263

https://insu.hal.science/insu-01574263

Submitted on 11 Nov 2020

HAL is a multi-disciplinary open access archive for the deposit and dissemination of scientific research documents, whether they are published or not. The documents may come from teaching and research institutions in France or abroad, or from public or private research centers.

L'archive ouverte pluridisciplinaire **HAL**, est destinée au dépôt et à la diffusion de documents scientifiques de niveau recherche, publiés ou non, émanant des établissements d'enseignement et de recherche français ou étrangers, des laboratoires publics ou privés.

Monthly Notices
of the
ROYAL ASTRONOMICAL SOCIETY

MNRAS **469,** S130–S141 (2017)
Advance Access publication 2017 June 9

doi:10.1093/mnras/stx1415

Organics in comet 67P – a first comparative analysis of mass spectra from ROSINA–DFMS, COSAC and Ptolemy

Kathrin Altwegg,[1,2★] H. Balsiger,[1] J.J. Berthelier,[3] A. Bieler,[1] U. Calmonte,[1] S.A. Fuselier,[4,5] F. Goesmann,[6] S. Gasc,[1] T. I. Gombosi,[7] L. Le Roy,[1] J. de Keyser,[8] A. Morse,[9] M. Rubin,[1] M. Schuhmann,[1] M. G. G. T Taylor,[10★] C.-Y. Tzou[1] and I. Wright[9]

[1]*Physikalisches Institut, University of Bern, Sidlerstrasse 5, CH-3012 Bern, Switzerland*
[2]*Center for Space and Habitability, University of Bern, Sidlerstrasse 5, CH-3012 Bern, Switzerland*
[3]*LATMOS 4 Avenue de Neptune F-94100 SAINT-MAUR, France*
[4]*Space Science Division, Southwest Research Institute, 6220 Culebra Road, San Antonio, TX 78228, USA*
[5]*University of Texas at San Antonio, 1 UTSA Circle, San Antonio, TX 78249, USA*
[6]*Max Planck Institute for Solar system Research, Justus von Liebig Weg 3, D-37077 Göttingen, Germany*
[7]*Department of Atmospheric, Oceanic and Space Sciences, University of Michigan, 2455 Hayward, Ann Arbor, MI 48109, USA*
[8]*Belgian Institute for Space Aeronomy, BIRA-IASB, Ringlaan 3, B-1180 Brussels, Belgium*
[9]*Department of Physical Sciences, The Open University, Walton Hall, Milton Keynes MK7 6AA, UK*
[10]*Science Support Office, European Space Research and Technology Centre, European Space Agency, NL-2201 AZ Noordwijk, the Netherlands*

Accepted 2017 June 6. Received 2017 April 28; in original form 2017 February 26

ABSTRACT

The ESA *Rosetta* spacecraft followed comet 67P at a close distance for more than 2 yr. In addition, it deployed the lander *Philae* on to the surface of the comet. The (surface) composition of the comet is of great interest to understand the origin and evolution of comets. By combining measurements made on the comet itself and in the coma, we probe the nature of this surface material and compare it to remote sensing observations. We compare data from the double focusing mass spectrometer (DFMS) of the ROSINA experiment on ESA's *Rosetta* mission and previously published data from the two mass spectrometers COSAC (COmetary Sampling And Composition) and Ptolemy on the lander. The mass spectra of all three instruments show very similar patterns of mainly CHO-bearing molecules that sublimate at temperatures of 275 K. The DFMS data also show a great variety of CH-, CHN-, CHS-, CHO_2- and CHNO-bearing saturated and unsaturated species. Methyl isocyanate, propanal and glycol aldehyde suggested by the earlier analysis of the measured COSAC spectrum could not be confirmed. The presence of polyoxymethylene in the Ptolemy spectrum was found to be unlikely. However, the signature of the aromatic compound toluene was identified in DFMS and Ptolemy data. Comparison with remote sensing instruments confirms the complex nature of the organics on the surface of 67P, which is much more diverse than anticipated.

Key words: comets: general – comets: individual: 67P/Churyumov–Gerasimenko.

1 INTRODUCTION

The surface of comet 67P/Churyumov–Gerasimenko is black with a very low albedo. The nature of this surface is the focus of remote sensing instruments like OSIRIS (Fornasier et al. 2015), VIRTIS (Capaccioni et al. 2015) and ALICE (Stern et al. 2015). Fornasier et al. (2015) reported a slightly reddish slope in the visible range with little absorption features. Capaccioni et al. (2015) reported a broad absorption feature at 2.9–3.6 μm that they associated with opaque minerals and a mixture of molecules composed of CH- and OH-bearing molecules and radicals with little nitrogenous contribution. In a more recent paper (Quirico et al. 2016), VIRTIS reported dark refractory polyaromatic material mixed with opaque minerals. The absorption feature at 3.2 μm they attribute to COOH in carboxylic acids. ALICE reported a slightly blueish slope in the ultraviolet wavelength range.

On 2014 November 12, the *Philae* spacecraft landed on the surface of comet 67P/Churyumov–Gerasimenko, thus making the first soft landing on a comet. *Philae* initially touched down

★ E-mail: altwegg@space.unibe.ch (KA); mtaylor@cosmos.esa.int (MGGTT)

© 2017 The Authors
Published by Oxford University Press on behalf of the Royal Astronomical Society

Downloaded from https://academic.oup.com/mnras/article/469/Suppl_2/S130/3865958 by guest on 11 November 2020

at the location called Agilkia, in the Máat region of the comet (Thomas et al. 2015) and following several bounces covering a trajectory of ∼1 km, finally came to rest at the Abydos site (Biele et al. 2015). On board *Philae* were two mass spectrometers, COmetary Sampling And Composition experiment COSAC (Goesmann et al. 2007) and Ptolemy (Morse et al. 2009): COSAC is a time of flight mass spectrometer coupled to a gas chromatograph, and Ptolemy is an ion trap mass spectrometer designed for detailed isotopic analysis. Both instruments were designed to analyse *in situ* cometary material brought up from the surface and subsurface by a drill (SD2; Finzi et al. 2007) but were also able to operate in a sniffing mode without active sampling from SD2. Shortly after *Philae*'s first touchdown, first Ptolemy and then COSAC performed preprogrammed measurement sequences in their sniff modes (Ulamec et al. 2016); they sampled cometary material most probably ejected from the Agilkia site during the touchdown, providing the first ever mass spectra so close to a comet (Goesmann et al. 2015; Wright et al. 2015). Further measurements were made; however, these initial spectra were noted to have the highest intensities and a number of peaks (Goesmann et al. 2015; Krüger et al. 2017) for the entire science operation period of *Philae* from 2014 November 12 to 15.

The Rosetta Orbiter Spectrometer for Ion and Neutral Analysis (ROSINA) with its two mass spectrometers – DFMS (Double Focusing Mass Spectrometer) and RTOF (Reflectron Time-Of-Flight) – and the Comet Pressure Sensor (COPS) onboard *Rosetta* (Balsiger et al. 2007) enjoyed a much longer operation period, analysing the cometary coma over a time period just greater than 2 yr. Their observations extended from a heliocentric distance of 3.6 au through perihelion and out again to 3.8 au before *Rosetta* finally also landed on the comet on 2016 September 30 at the Sais site, in the Ma'at region of the comet. It should be noted that *Rosetta* operations ceased immediately on impact in the Sais, so there are no ROSINA data from the surface of the comet. During the final phases of the mission, *Rosetta* was gradually reducing pericentre distances and on 2016 September 5, *Rosetta* flew at less than 2 km above the surface of the comet. During this pericentre crossing, ROSINA–COPS reported very high density spikes lasting several minutes, in addition to the star trackers experiencing significant difficulties in attaining tracking of stars for navigation purposes. Several of other science instruments reported a significant enhancement of the dust environment, with the GIADA instrument observing values equivalent to a previous large outburst event on 2016 February 19 (A. Rotundi, private communications). Unlike the 19 February event however (Grün et al. 2016), which was more refractory dominated, the September event was more akin to the impact of a 'chunk' of ice and dust from the comet, containing refractory and semivolatile material. The amount of material entering the ionization box of DFMS must have been large and solid, as it blocked physically for some time the electron path between filament and electron trap, almost leading to the destruction of the filament. And the event lasted for a long time seen with COPS and Giada. The S/C was far from Sun at 3.8 au, but close to the comet. The velocity of the grains was ∼4 m s^{-1} (A. Rotundi, principal investigator of the GIADA instrument, private communication) and therefore the flight time from the comet surface to the spacecraft short (∼500 s). This means that most semivolatiles did not reach temperatures to sublimate before the start of the measurements. Unfortunately, the RTOF component of ROSINA, which has a high time resolution, was not operating due to power restrictions but ROSINA–DFMS recorded mass spectra during this time in a high-resolution mode from mass 13 Da to mass 100 Da, yielding an enormous wealth of mass peaks over the whole mass range.

All three mass spectrometers (entire ROSINA, COSAC and Ptolemy) are designed to measure sublimating gases. None was able to measure directly refractory dust. However, it turned out that the carbonaceous material seen by the remote sensing instruments is at least partly volatile at elevated temperatures around 275 K, which makes it accessible to all three mass spectrometers. Although the way how and where this material was collected differs from sensor to sensor, the results are nonetheless comparable. In this paper, we compare the results from all three mass spectrometers in order to get a coherent picture of 67P's semi-volatile surface material.

2 METHOD AND OBSERVATIONS

2.1 Mass spectrometry and fragmentation

Mass spectrometry of a neutral gas requires the constituent molecules to be ionized, most commonly by electron impact ionization. In the case of COSAC and Ptolemy, this is done with 70 eV electrons and in the case of DFMS, the ionization energy used is only 45 eV. This process not only produces the ionized parent species but in the case of molecules also some ionized daughter species, called fragments. The fragmentation pattern (the relative abundances of the individual peaks) depends very much on the electron energy as well as on the structure of the molecule to be ionized. This can be very helpful, as it allows different isomers to be distinguished due to their different molecular structure and hence binding energies. It also means that molecules can be excluded based on missing fragments. On the other hand, it makes mass spectra very complex with one parent molecule often yielding many mass peaks. Also, especially for more complex organics, the ionized parent is very often not the highest peak in the spectrum and can furthermore be a daughter species of yet another, higher mass molecule. In most cases, when saturated species fragment they end up as two radicals/ions. Only in very special cases can a rearrangement during fragmentation of a saturated molecule/ion result in the production of another (lower mass) saturated molecule. Thus, even though the fragmentation patterns of alkanes are very similar, stoichiometry dictates that an ionized saturated molecule (i.e. a species with only single bonds) can only be due to a parent and not a fragment, e.g. $C_3H_8^+$ arises from propane (C_3H_8) and not a higher hydrocarbon. Further examples include CH_4O^+ (ionized methanol, which can only arise from methanol itself) and $C_3H_9N^+$ (ionized C_3H_9N, which could arise from any of the structural isomers of this compound, e.g. propylamine, trimethylamine, methylethylamine, etc., but not a higher hydrocarbon such as $C_4H_{11}N$). For species containing double and triple bonds, the situation is more complicated, as the same peak could be a parent or a fragment of a heavier species. This then needs a look at the whole mass spectrum to assess contribution of heavier species to lighter ones. A good knowledge on fragmentation patterns for the specific instrument parameters is therefore mandatory. However, sometimes this is not easily achieved as some compounds are highly poisonous, corrosive or unstable, making their usage in the laboratory very difficult. The National Institute of Standards and Technology (NIST; Stein 2016) provides a data base of mass spectra for many such compounds, usually taken with mass spectrometers at unit mass resolution. Using different mass spectrometers (e.g. time-of-flight, magnetic or orbitrap instruments) may give fragmentation patterns with deviating relative peak heights due to mass-dependent fractionation inside the sensors. For example, ROSINA–DFMS cannot be directly compared to the NIST data base due to the different electron energy and the mass-dependent sensitivity, but for qualitative analysis the general fragmentation

Downloaded from https://academic.oup.com/mnras/article/469/Suppl_2/S130/3865958 by guest on 11 November 2020

pattern is similar between NIST and DFMS (Stein 2016). At lower electron energies, molecules tend to fragment to a lesser extent, yielding a relatively higher signal for the ionized parent molecules and smaller signals for fragments. This can be seen in the spectrum of heptane in Appendix A, where the NIST fragmentation pattern is compared to the measured DFMS fragmentation pattern. Differences in relative abundances are on the order of 30 per cent.

2.2 The DFMS mass spectrometer

DFMS is a classical mass spectrometer with a Nier–Johnson configuration (Balsiger et al. 2007). It consists of a toroidal electrostatic analyzer selecting the energy of the ions followed by a permanent magnet selecting the momentum. DFMS has two entrance slits in front of the electrostatic analyzer, one with 14 μm slit width and the other one with 200 μm that can be selected by deflecting the ion beam. In this study only the narrow slit that gives a high mass resolution was used. The entrance slit is mapped on to a multichannel plate (MCP) with a position sensitive linear anode containing two (for redundancy reasons) rows with 512 pixels each (Nevejans et al. 2002). Because the pixel size is 25 μm, the image of the entrance slit is enlarged by an ion optical zoom between magnet and detector consisting of two electrostatic quadrupoles and a hexapole. The zoom is set to 6.4 for the high-resolution mode for the mass range considered here. The relation between pixel x and mass m is given by $m = \exp((x - x0) \times d/(z \times \mathrm{disp})) \times m0$, d being the pixel size, z the zoom factor, disp the dispersion constant of the magnet (=0.127 m) and $m0$ the commanded mass that falls on to pixel $x0$, near the centre of the MCP. The position of this central pixel can be chosen by the voltage settings of the electrostatic analyzer. It was shifted after some time into the mission to a new location by command because the detector slowly was degrading around this centre location, but it was always kept within 50 pixels of the centre pixel 256 where the mass resolution is largest. This means that a mass range of approximately ±0.22 Da for e.g. mass 28 Da and ±0.53 Da for mass 60 Da is measured simultaneously. For mass 28 Da, 1 pixel difference corresponds to 0.000 85 Da, and for mass 60 Da, it is 0.001 85 Da. Whereas the zoom factor and the dispersion are almost temperature independent and very well known for the whole mass range, $x0$ can drift with temperature due to the temperature dependence of the magnetic field. This is minimized by constant measurement of the magnet temperature and voltage readjustment. In addition, this temperature drift is slow, less than 1 pixel per 30 min (time needed to measure 60 masses), once the instrument is in thermal equilibrium. So-called anchor peaks are used to determine $x0$ very precisely. These are peaks that were always present in the mass spectrum, including species observed even before *Rosetta* arrived at the comet, from S/C outgassing (e.g. water, CO, CO_2), and those arising from many cometary species/fragments like C_2, the triplet on mass 32 Da (S, O_2, CH_3OH) and CS_2. DFMS peaks can be well described by double Gaussians, where the centre is the same for both, the width of the second one is about three times the width of the first one and the height of the second one is around 10 per cent of the major one. This leads then to a mass determination on subpixel level, which is better than 0.001 Da, if needed. DFMS has a high mass resolution of $m/\Delta m = 9000$ at mass 28 Da. This high resolution, together with the precise mass determination, can then be used to separate different species/fragments on the same integer mass, which is hardly possible with the other mass spectrometers flown on *Rosetta* (ROSINA RTOF) and *Philae* (COSAC and Ptolemy). DFMS also has a very high sensitivity, with a dynamic range of up to 10^{10} (Balsiger et al. 2007).

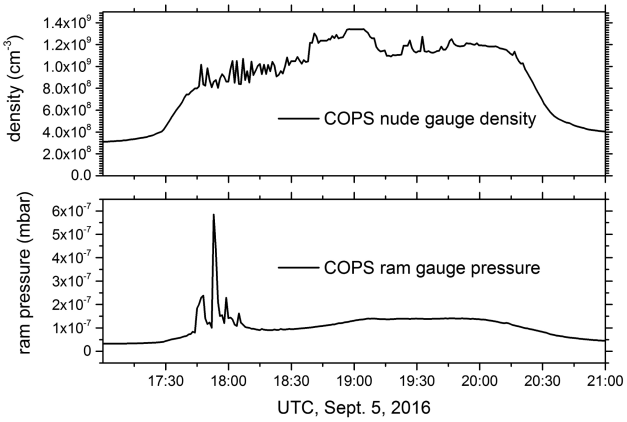


Figure 1. COPS measurements on 2016 September 5. Top: total density, bottom: ram pressure.

The flight model of DFMS underwent basic calibration before flight where all important parameters were determined and voltages optimized. However, the number of compounds used for this calibration was limited on purpose in order not to leave terrestrial contamination in the instrument. Compounds used included Ne, CO_2 and Xe, which cover with their fragments the full mass scale of DFMS. There exists, however, an identical twin instrument in the laboratory, which was/is extensively used for calibration purposes, especially to determine fragmentation patterns, using the calibration facility CASYMIR (CAlibration SYstem for the Mass spectrometer Instrument ROSINA; Graf et al. 2004). Gaseous compounds as well as liquids and solids with a relatively high vapour pressure can be inserted into the vacuum chamber either in a static mode with a fixed partial pressure or as a molecular beam, thus simulating the outgassing of the comet.

In this paper, we consider the material sampled by DFMS during 2016 September 5 as the best analogue to the material sampled by COSAC and Ptolemy at the comet surface. We compare the three data sets with an aim to improve on the initial analysis carried out on the COSAC and Ptolemy data sets.

2.3 The 2016 September 5 event and ROSINA data

In the last few weeks of the mission before landing on the comet, *Rosetta* flew elliptical orbits with the pericentre lowered gradually and the apocentre increased, keeping the size of the ellipse constant. On 2016 September 5 around 22h UTC it reached its closest distance from the comet, 3.9 km from the comet centre (approximately 1.9 km above surface). At that time, *Rosetta* was at the equator coming from the southern (winter) hemisphere. About 5h earlier, *Rosetta* was most probably hit by a chunk of ice and dust, showing high-density peaks for more than 3 h in the vicinity of the ROSINA–COPS nude gauge with its FOV of 340° (Fig. 1, top).

Around 19 h the nude gauge even was in saturation. The COPS ram gauge, measuring ram pressure and pointing towards the comet, shows large hits around 18 h, most likely dust–ice grains entering the equilibrium chamber (Fig. 1, bottom, cf. Balsiger et al. 2007) and sublimating inside the gauge.

ROSINA–DFMS also registered the likely impact to its ionization box of a large amount of cometary material at the same time and coincidently, DFMS had just started a measurement sequence from mass 13 Da to mass 50 Da and then a second one from mass 44 Da to mass 100 Da. The temperature of the ionization box was 1°C–2°C throughout the measurement period, allowing semivolatile material

Downloaded from https://academic.oup.com/mnras/article/469/Suppl_2/S130/3865958 by guest on 11 November 2020

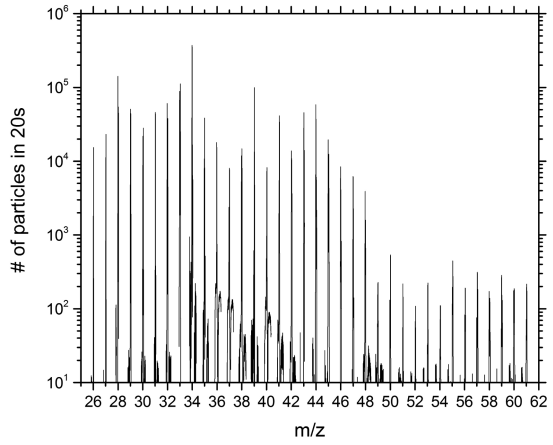


Figure 2. DFMS mass spectra in high resolution between 1803 h and 1853 h UTC on 2016 September 5.

to slowly sublimate. DFMS, contrary to time-of-flight instruments, measures masses sequentially. Each integer mass has 20 s integration time plus an additional 10 s for adjusting voltages and detector gain. That means it took roughly 50 min to go from mass 13 to mass 100 Da. Throughout this period, signals were high, but decreasing with time. Water was measured at the beginning, in between the two sequences and at the end. From beginning to end, water decreased by about a factor of 5.

Fig. 2 shows the DFMS data from mass 26 Da to mass 62 Da. There is a clear peak on every mass number. The vertical axis is the number of registered ions on the detector during the integration time of 20 s. The sensitivity of DFMS drops in the mass range considered proportional to $m^{-0.8}$ due to the energy-dependent transmission and detector yield. For a quantitative analysis, this instrument specific sensitivity and the ionization cross-section together with the fragmentation pattern of the individual species have to be taken into account. However, as pointed out in the Introduction section, qualitatively NIST and DFMS (Stein 2016) fragmentation patterns are similar. To facilitate a comparison between instruments, Fig. 3 shows a zoom of all DFMS peaks from September 5 coincident with the COSAC data peaks observed from 2014 November 12 (and detailed in the next section). The figure immediately demonstrates the complexity of the composition of the comet. On most masses above 29 Da, there are five or more individual peaks, each belonging to one or several parent species. In some cases, there is clearly a major peak, being larger by at least a factor of 3 than the other peaks on the same integer mass. But very often, there are at least two peaks with similar intensities.

Fig. 4 shows the results sorted by involved functional groups of atoms and the possible parent molecules. Abundances strongly decrease with mass, therefore limiting contribution of heavier molecules to lighter ones. Starting with hydrocarbons, the DFMS results are compatible with a mixture of ethane, propane and butane. Ethane has the highest peak on mass 28 Da, propane on mass 44 Da and butane on mass 43 Da. The high peak on mass 39 is partly, but not only due to contributions from propane and butane. Some heavier hydrocarbon chains, probably from unsaturated molecules, also contribute to the fragments. This is in line with the carbonaceous matter found in the dust of C-G by the COmetary Secondary Ion Mass Analyser (COSIMA), which identified signatures of CH-bearing macromolecules (Fray et al. 2016).

CHO-bearing molecules are generally abundant in the spectra. Methanol, together with formaldehyde, fits very well the fragmentation pattern CH_nO (n=1–4) with the highest peak of methanol on mass 31 Da, of formaldehyde on mass 29 Da. One must consider that these DFMS observations are not only of the chunk of impacting ice and dust, but also the ambient coma gases. It is therefore not surprising that for mass 28 Da, CO is the dominating species. Part of CO is a fragment of CO_2, but the undisturbed coma contains a significant amount of CO (e.g. Hässig et al. 2015). The peaks on masses 46 and 45 Da (C_2H_6O and C_2H_5O) fit very well ethanol and mass 44 Da (C_2H_4O) contains another fragment of ethanol, but also some acetamide, as the peak is too high to only be a fragment of ethanol. The C_2H_2O peak is very high, likely containing fragments from larger CHO-bearing molecules, and the series of C_3H_nO shows the typical fragmentation pattern of propanol, with a low signal on the parent species, but a specific pattern with higher peaks on the odd masses 53, 55, 57 and 59 Da compared to the even numbered masses. C_3H_6O is too large to be accounted for by propanol only. Acetone is a possible contributor and would then also contribute to the high peak on mass 43 Da. Propanal cannot be excluded, but it would only be a small contribution as it does not produce the fragmentation pattern seen between masses 53 and 59 Da. The possibility is high that also longer chains of (unsaturated) CHO-bearing molecules are contributing to the mass range considered here. A full inventory of CHO-bearing molecules will be the subject of subsequent papers, following a thorough calibration campaign.

CHS-bearing molecules are the third most abundant species. Thioformaldehyde and methanethiol are quite abundant and account for e.g. almost 50 per cent of the peak at mass 45 Da (CHS). Longer chain CHS-bearing molecules are also detected, whereby it is not possible to state without detailed analysis if the parent is dimethylsulphide or ethanethiol, two isomers with the chemical formula C_2H_6S. DFMS also measures H_2S and SO/SO_2, which are abundant in the gas phase and are likely due to the ambient coma. These molecules produce substantial amounts of S^+ upon electron impact ionization, contrary to the organo-sulphurs, which is also observed in the DFMS spectra.

A similar pattern to the hydrocarbons can be seen for the CHN-bearing molecules. Hydrogen cyanide is quite prominent and methylamine, ethylamine and propylamine are clearly identified from their ionized parents at masses 31, 45 and 59 Da, respectively. All three species are singly bonded saturated molecules that cannot be fragments of heavier molecules (but which could include contributions from their isomers). The ionized parent species are smaller than the fragments, which are in line with the NIST fragmentation pattern. Whether acetonitrile (CH_3CN) is present is difficult to say without a careful calibration of the fragmentation patterns of the amines and acetonitrile. It cannot be the major species in the C_2H_nN-bearing group as it would by far not produce enough of C_2NH_2 and C_2NH. Overall the abundance of CHN-bearing molecules is rather small compared to the CH- or CHO-bearing molecules, in line with comets being depleted in N-bearing species (Rubin et al. 2015).

Of course, SO_2 is abundant as it is not only in the ice–dust mixture, but also in the ambient coma at the time of the measurements. CHO_2-bearing molecules have a similar abundance as the CHN-bearing molecules, but are clearly seen in the DFMS spectra. Formic acid and acetic acid fit the fragmentation pattern for shorter CHO_2-bearing chains. Ethylene glycol or dimethyl peroxide seems to be present as well shown by the peak on mass 62 Da. Longer (unsaturated) CHO_2-bearing chains are likely to be present as with the aforementioned molecules alone the fragmentation pattern cannot be satisfied. In particular, the fragments on masses 47–49 Da are due to heavier CHO_2 molecules. CHNO-bearing molecules are

Downloaded from https://academic.oup.com/mnras/article/469/Suppl_2/S130/3865958 by guest on 11 November 2020

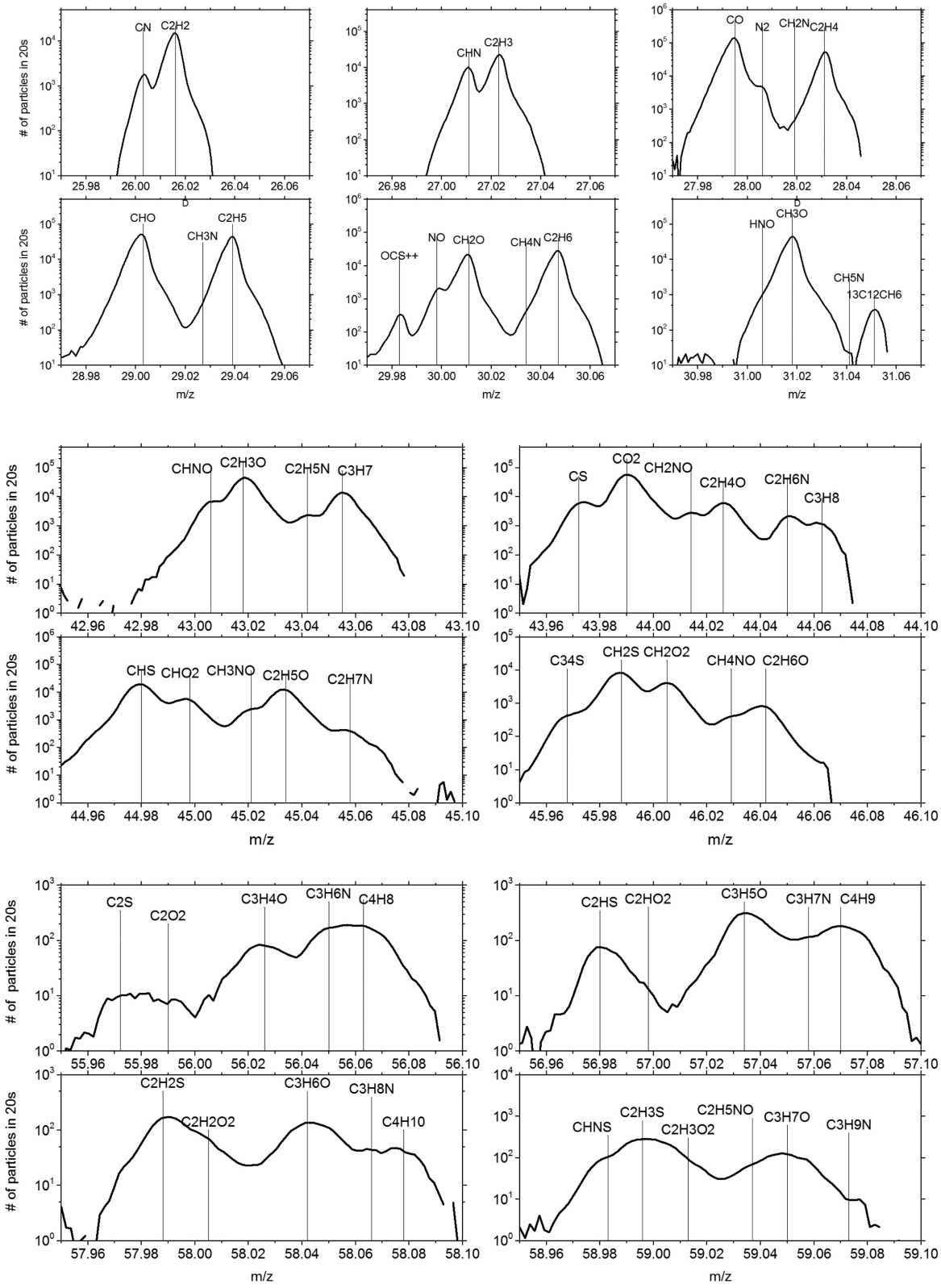


Figure 3. Single DFMS mass spectra, zoomed in. Indicated are the nominal positions of the individual species/fragments.

present roughly at the 10 per cent level of the CHO-bearing species. CHNO, isocyanic acid, is very likely one of the major CHNO-bearing molecules together with formamide. A small amount of acetamide is most probably present, but no methyl-isocyanate or its isomers. Again, it is very likely that heavier CHNO-bearing molecules are contributing as well. Finally, masses 32–41 Da in the DFMS spectra are likely to contain H_2S, O_2, O_2H, O_2H_2 and hydrocarbon fragments.

Downloaded from https://academic.oup.com/mnras/article/469/Suppl_2/S130/3865958 by guest on 11 November 2020

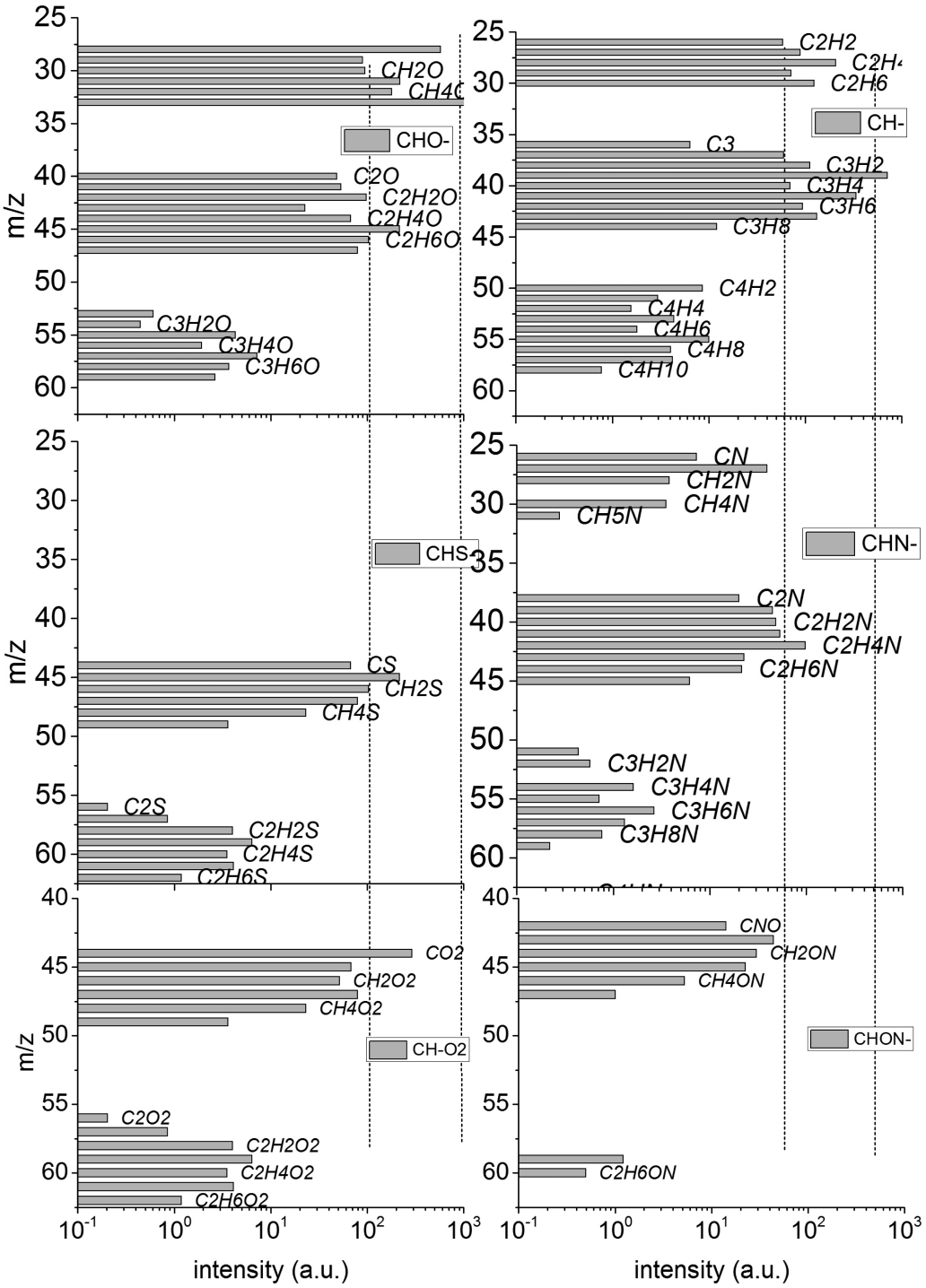


Figure 4. Intensities of measured DFMS peaks. The intensities are not corrected for the specific instrument sensitivity and also not for the change in overall gas density. For readability, only fragments with an even number of hydrogens are labelled.

Using these new measurements from ROSINA as proxies for near surface cometary material, we revisit the COSAC and Ptolemy observations of 2014 November 12.

2.4 Re-visiting the COSAC data

Fig. 5 shows the COSAC data taken from Goesmann et al. (2015). The time of flight section of COSAC has a theoretical mass resolution $m/\Delta\, m$ of ∼300. This should allow a mass peak determination of better than 0.01 Da for masses at ∼44 Da, as the centre of a peak is more precise by up to a factor of 10 than the full width at half-maximum. However, in order to improve counting statistics (Goesmann et al. 2015) accumulated the counts in 1 Da resolution bins centred around integer mass numbers thus reducing the mass resolution. The dashed line denotes the intensity below which measured counts cannot be distinguished from background as there are no visible peaks for those masses in the COSAC mass spectrum. Goesmann et al. (2015) used a superposition of standard NIST mass

Downloaded from https://academic.oup.com/mnras/article/469/Suppl_2/S130/3865958 by guest on 11 November 2020

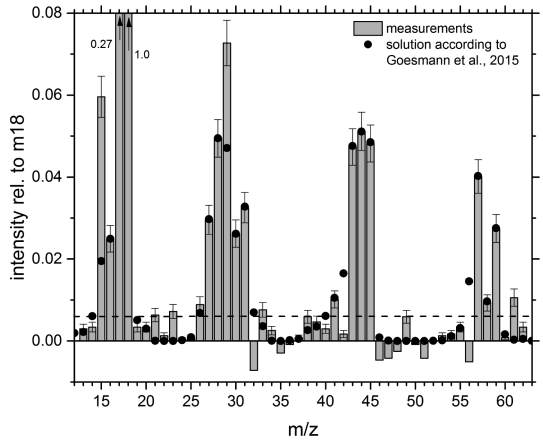


Figure 5. The COSAC mass spectrum according to table S-2, supplementary material of Goesmann et al. (2015), normalized to mass 18 Da, together with the fitted spectrum (black dots), according to Goesmann et al. (2015).

(Stein 2016) spectra of candidate cometary molecules to find a best fit for the observed COSAC spectrum, and particularly focused on reducing as much as possible the number of species required for that fit. Starting from 59 Da (and not considering any peaks in the range $>$ 62 Da), the fit was made in order of decreasing mass to allow for the contributions of fragmentation from heavier molecules to be accounted for at lower mass. Additional molecules were also introduced in these bins in cases where signal intensity needed to be enhanced. The most unstable species and the organic molecules with unsaturated carbon–carbon bonds were avoided. They combined this reduction approach to fitting with plausible formation pathways (Fig. 3; Goesmann et al. 2015) to conclude with a spectrum (black dots) including 16 different parent molecules. This list of molecules is given in Table 1, including four (in bold) that had never previously been detected in comets.

In the far-right column of Table 1, we indicate which of the Goesmann et al. (2015) molecules have been identified in the DFMS spectra and which have not. As presented above, the DFMS spectrum shows significant complexity and suggests that the strategy of minimizing the number of molecules in the fit implemented by Goesmann et al. (2015) and the related chemistry discussion may require modification. In addition, the DFMS data seem to indicate that unsaturated molecules could play an important role in the carbonaceous matter of 67P. The exclusion of such species may have to be reconsidered as well. Immediately this leads us to reconsider the model composition for masses 42 Da (fragment from acetamide) and 56 Da (from methyl isocyanate), which as shown in Fig. 5 is high, yet the COSAC measurements show almost no or even negative counts after subtraction of the background. On the other hand, there are the peaks at masses 29 and 15 Da, respectively, which are only partially accounted for, well outside the 2σ and 3σ confidence limits, respectively.

We revisit the COSAC data at the full mass resolution, with reduced counting statistics, by fitting all mass peaks seen in the raw data with one Gaussian per integer mass. A determination of the mass centre to within 0.01 Da allows including/excluding species.

The result is shown in Fig. 6 and Table 2.

For a time of flight mass spectrometer, the mass m is given by $m = c(t - t_0)^2$. c is given by the specific geometry of the instrument and by the energy of the ions, t is the flight time and t_0 accounts for a shift of the start pulse relative to the actual start time. Knowing two peaks with the exact mass in the spectrum allows determining these two parameters. In the case of the COSAC spectrum (Goesmann et al. 2015), the authors assume H_2O for mass 18 Da and CO_2 for mass 44 Da (although mass 44 Da was in the end not associated with CO_2, this does not play a role as long as the counts are binned as done in their paper). Fitting mass 18 Da shows that the real mass resolution is $\sim$220, only slightly lower than the theoretical one of 300 (Goesmann et al. 2015). It also shows that a simple Gaussian is a good approximation for the COSAC peak shape. Fitting the individual peaks depends on an accurate mass scale. For example, if instead of assigning the peak at mass 44 Da to CO_2, we use a combination of acetaldehyde and the fragment of acetamide, we assign a mass of 44.020 Da to the peak centre in order to calculate c and t_0. This then shifts the centre masses for masses 30 and 57 Da to masses 30.062 and 57.073 Da, respectively, which are inconsistent with any possible species or fragments. We therefore conclude that mass 44 Da is dominated by CO_2 in accordance with the original mass scale applied by Goesmann et al. (2015). If CO_2 is assigned

Table 1. Parent molecules used for fitting the COSAC spectrum according to Goesmann et al. (2015). Species in bold have never before been identified in a comet. The last column indicates which of the molecules have been identified in the ROSINA–DFMS spectra during the 2016 September 5 event.

Molecule		Mass (Da)	Rel. abundance (per cent)	Identified in DFMS spectra
CH_4	Methane	16	0.7	Y
H_2O	Water	18	80.9	Y
CHN	Hydrogencyanide	27	1.1	Y
CO	Carbon monoxide	28	1.1	Y
CH_5N	Methylamine	31	1.2	Y
CH_3CN	Acetonitrile	41	0.5	minor
CHNO	Isocyanic acid	43	0.5	Y
C_2H_4O	Acetaldehyde	44	1.0	Y
CH_3NO	Formamide	45	3.7	Y
$C_2H_5NH_2$	Ethylamine	45	0.7	Y
CH_3NCO	**Methyl isocyanate**	57	3.1	
C_3H_6O	**Acetone**	58	1.0	Y
C_2H_5CHO	**Propanal**	58	0.4	?
CH_3CONH_2	**Acetamide**	59	2.2	minor
CH_2OHCHO	Glycol aldehyde	60	1.0	
$CH_2(OH)CH_2(OH)$	Ethylene glycol	62	0.8	Y

Downloaded from https://academic.oup.com/mnras/article/469/Suppl_2/S130/3865958 by guest on 11 November 2020

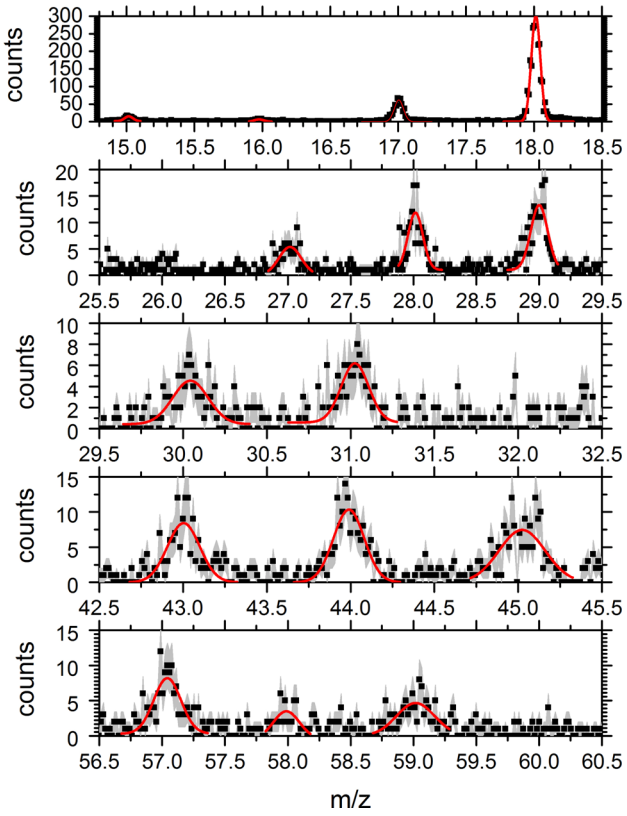


Figure 6. The COSAC raw data with a Gaussian fit.

to mass 44 Da, this then produces some CO by fragmentation and is more consistent with other CO_2/CO values (e.g. Morse et al. (2015)).

In Table 2, alongside their integer mass, in bold are species whose exact mass is within 1 σ of the fitted peak centre shown in column 4. Also given are the calculated mass resolution and in the last column the relative peak heights contributing to a single integer mass as deduced from the DFMS spectra discussed later in the paper. Considering the mass peaks in Table 2, some peaks have a comparable mass resolution to water (thus are likely dominated by one species), while others are lower (suggesting that the peak is a result of two different mass species). The 1σ error in the peak centre is below 0.02 Da for most species and mass 58 Da has a very poor fit due to the low count rate. Masses not shown in Table 2 do not exhibit any visible peak above background in the raw data.

Using Table 2, we can include/exclude some more species being major contributors to the COSAC spectrum: CO, acetaldehyde and acetone are most likely not major contributors to the measured peaks as their masses are outside of the 1 error of the fitted mass peak.

Most species contributing to the mass spectrum of COSAC are CHO-containing species according to the fitted mass peaks, with mass 44 dominated by CO_2 and some N-bearing species in lesser concentrations, contrary to Goesmann et al. (2015), who assigned the highest contribution to the COSAC nitrogen-bearing molecules. However, 67P has been shown to be depleted in the major N-bearing molecules N_2 and NH_3 (e.g. Rubin et al. 2015) and as indicated above, the DFMS spectra also showed depletion. The mass differences between the group of peaks around 59 and 44 Da are compatible with -CH_2- or -O- addition/loss. On mass 30 Da, only ethane (C_2H_6) can explain the centre peak position.

Overall the COSAC spectrum shows great similarities to that observed by DFMS, and as noted above, given the complexity of the DFMS spectra overall, we should reconsider the chemistry discussion and the overall fit of the features of the COSAC spectrum from Goesmann et al. (2015). In this case, methyl isocyanate cannot be the dominant molecule on mass 57 Da (false-positive detection due to the missing fragment at mass 56 Da) and acetamide must also likely be excluded for 59 Da, due to the lack of a peak on 42 Da. We also reconsider the presence of glycol aldehyde, due to the lack of a peak at mass 32 Da. We note that the absence of a peak around 32 Da does not exclude the existence of sulphur-bearing species as organo-sulphur (CH_2S, CH_4S, C_2H_6S) and CS_2 fragmentation patterns do not produce significant amounts of S^+ (e.g. Calmonte et al. 2016).

2.5 Re-visiting the Ptolemy data

To compare data from Ptolemy to COSAC or ROSINA data is not easy as the ionizing energy of the 70 eV electron beam is modified by the RF voltage of the ion trap. Furthermore, ions are then stored for at least 1 ms. This storage can lead to protonation and ions can then appear in the mass spectrum at one mass number higher than their original mass. For a qualitative analysis, Ptolemy mass spectra are in general similar to NIST mass spectra, in conditions with low levels of hydrogen or water. At high concentrations of hydrogen or water, CO_2, N_2 and CO (whether from a molecule of CO or from CO_2 fragmentation) are known to protonate, whilst O_2 does not; these were the target molecules of interest for isotopic analysis by Ptolemy. Wright et al. (2015) identified mass 45 Da as coming mostly from protonated CO_2 and suggested that the periodic pattern in their mass spectrum with repeating units of 16:14 *m/z* indicates an -O- and -CH_2- addition/loss. A similar pattern was found by the PICCA (Positive Ion Cluster Composition Analyser) instrument (Korth et al. 1986) during the Giotto Halley flyby in 1986. At that time, this pattern was identified as being compatible with polymerized formaldehyde, also referred to as polyoxymethylene (POM) ($(CH_2O)_n$) (Huebner 1987). This was also in line with a distributed source for formaldehyde and CO (Meier et al. 1993), which means that formaldehyde and CO were in part released not only from the nucleus, but also from dust grains in the coma. Later, however, it was shown by Mitchell et al. (1989) that this pattern is generally characteristic of organic molecules composed of carbon, hydrogen and oxygen (CHO- molecules). In addition, Rubin et al. (2011) showed that the distributed sources could also be explained by temporal variations in the outgassing rate of the comet. POM is therefore not needed to explain PICCA data or distributed sources for formaldehyde, although work done on cometary analogues by Cottin et al. (2004) showed that POM can easily be synthesized in a cometary environment. The question therefore remains whether POMs are an important component of comets and whether synthesis of complex organics contributes to part of the dark colour of comets. POMs are solid for temperatures below 15°C, but sublimate at higher temperatures. In order to investigate the presence of POMs, the ROSINA flight spare instrument was therefore calibrated with commercially available polyoxymethylene ($HO(CH_2O)_nH$, CAS Number: 30525-89-4, MDL: MFCD00133991) in the laboratory in order to quantify the fragmentation pattern of POM. POM was thermally desorbed at temperatures below 40°C in our calibration chamber CASYMIR that was connected to either ROSINA–DFMS or ROSINA–RTOF. The results were very similar for both instruments.

Fig. 7 shows a typical RTOF spectrum of POM. RTOF is a time-of-flight instrument, with a similar ionization source as COSAC

Downloaded from https://academic.oup.com/mnras/article/469/Suppl_2/S130/3865958 by guest on 11 November 2020

Table 2. Result of peak fits of the raw COSAC data from Goesmann et al. (2015). The first column indicates the integer mass of the peak, and the next two columns indicate the possible species contributing to this integer mass with their exact mass. In bold are species that are compatible with the fitted peak position within 1. The last column shows the relative abundances of the different species to the corresponding integer mass as seen in the DFMS spectra.

Integer mass	Species	Exact mass	Peak centre	$\pm1\sigma$	$m/\Delta\, m$	$\pm1\sigma$	Rel. abundance DFMS
15	NH	15.01					1 per cent
	CH_3	15.023	15.017	0.002	206	24	99 per cent
16	O	15.994	15.976	0.012	192	34	89 per cent
	NH_2	16.018					3 per cent
	CH_4	16.03					8 per cent
17	OH	17.002	17.005	0.002	221	13	98 per cent
	NH_3	17.026					2 per cent
18	H_2O	18.01	18.012	0.002	228	10	100 per cent
27	HCN	27.01	27.017	0.011	135	20	30 per cent
	C_2H_3	27.022					70 per cent
28	CO	27.994					71 per cent
	N_2	28.006	28.016	0.017	200	26	3 per cent
	CH_2N	28.018					1 per cent
	C_2H_4	28.031					25 per cent
29	CHO	29. 002	29.001	0.007	181	19	66 per cent
	C_2H_5	29.038					34 per cent
30	OCS^{2+}	29.983					1 per cent
	NO	29.997					4 per cent
	H_2CO	30.01					40 per cent
	CH_4N	30.033	30.043	0.01	167	19	2 per cent
	C_2H_6	30.046					53 per cent
31	CH_3O	31.017	31.026	0.008	163	27	99 per cent
	CH_5N	31.041					1 per cent
43	CHNO	43.005	43.003	0.011	189	22	7 per cent
	C_2H_3O	43.017					68 per cent
	C_2H_5N	43.041					4 per cent
	C_3H_7	43.054					21 per cent
44	CS	43.972					14 per cent
	CO_2	43.99	43.99	0.007	202	15	60 per cent
	CH_2ON	44.013					6 per cent
	C_2H_4O	44.027					13 per cent
	C_2H_6N	44.049					4 per cent
	C_3H_8	44.062					3 per cent
45	CHS	44.979					48 per cent
	CHO_2	44.997					15 per cent
	CH_3ON	45.02	45.023	0.017	141	18	5 per cent
	C_2H_5O	45.033					31 per cent
	C_2H_7N	45.057					1 per cent
57	C_2HS	56.979					6 per cent
	C_3H_5O	57.033	57.042	0.011	233	23	52 per cent
	C_2H_3NO	57.051					0 per cent
	C_3H_7N	57.054					9 per cent
	C_4H_9	57.069					31 per cent
58	C_2H_2S	57.987	57.99	0.018	237	197	39 per cent
	$C_2H_2O_2$	58.005					10 per cent
	C_3H_6O	58.041					36 per cent

(Balsiger et al. 2007) that takes a full mass spectrum in one measurement similar to the sniff mode of COSAC. Background was subtracted as well as residual gas. However, by introducing and thermally desorbing POM, also some water was released into the vacuum chamber and is seen in the spectrum. The monomer, formaldehyde with its fragmentation pattern can easily be seen between masses 28 and 31 Da. The dimer around mass 60 Da is reduced by 3 orders of magnitude. The trimer on mass 91 Da is hidden in the noise. Looking at this fragmentation pattern, it is clear that thermal desorption of POM produces mostly the monomer, only very little dimer or longer chains and it does not produce the observed periodic pattern with repeating units of 16:14 m/z that is typical of CHO-bearing species. These ROSINA RTOF POM results are not compatible with the suggestion by Wright et al. (2015) that POM is responsible for the high peak on mass 91 Da as well as the peaks between 55 and 60 Da.

Downloaded from https://academic.oup.com/mnras/article/469/Suppl_2/S130/3865958 by guest on 11 November 2020

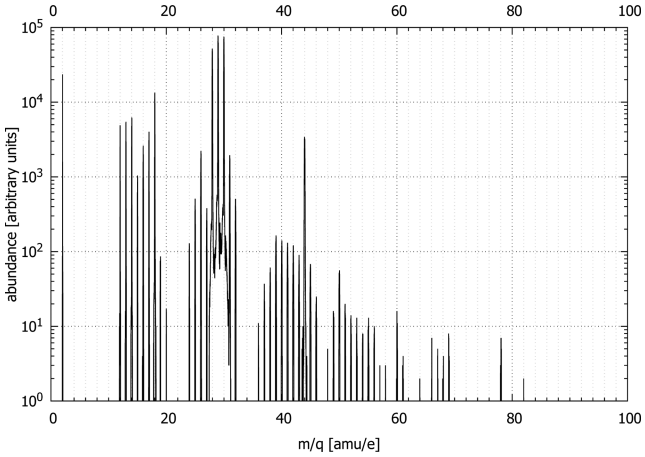


Figure 7. The ROSINA–RTOF spectrum of commercially available polyoxymethylene (paraformaldehyde) thermally desorbed in vacuum.

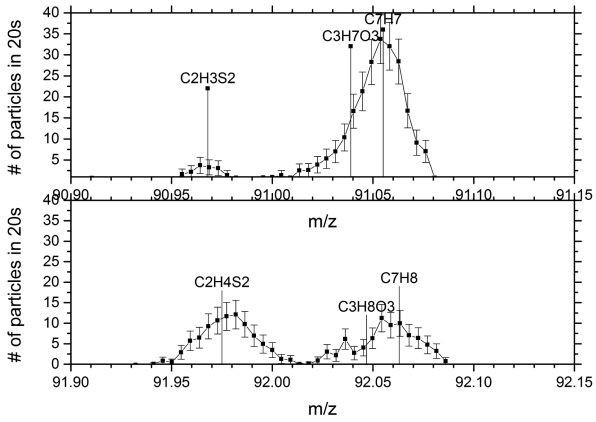


Figure 8. The DFMS mass spectra of masses 91 and 92 Da, showing the fragmentation pattern of toluene.

Ptolemy has a high peak on mass 33 Da, which is also seen in the DFMS data discussed previously (e.g. Fig. 7). For DFMS this peak is due to HS (∼50 per cent) and to CH_5O (50 per cent). For DFMS, CH_5O is probably protonated methanol due to the very high water density in the ion source of DFMS at that time. Due to the different ionization with subsequent storage of the ions of 1 ms in Ptolemy, the same could be true as methanol protonates readily similar to H_2O or CO_2.

DFMS also measured masses 91 and 92 Da, where there are quite high peaks in the Ptolemy spectrum. The spectra are in Fig. 8. While the peaks to the left are due to complex sulphur-bearing species, with the parent not yet identified, the peaks to the right are clearly due to C_7H_7 and C_7H_8.

Their intensity distribution is compatible with toluene. Toluene has been observed in many DFMS mass spectra during the mission and seems to be relatively abundant. The intensity distribution is also compatible with the Ptolemy spectrum. We therefore conclude that the peaks on masses 91 and 92 Da in the Ptolemy spectrum are most probably due to toluene and not to polyoxymethylene-trimer and glycerol, respectively. According to the NIST data base, glycerol yields hardly any ionized parent molecule upon electron impact ionization, but just fragments below mass 75 Da. Considering the DFMS observations discussed above, the global pattern of the spectra in Wright et al. (2015) is likely predominantly due to CHO-bearing molecules, probably with some minor nitrogen-bearing molecules added. Due to the lack of signal on mass 32 Da, as with Goesmann et al. (2015), sulphur-bearing species were not considered. Overall, the results of COSAC and Ptolemy are compatible with one another, even if relative abundances of the peaks are different. Some of these differences are due to the different kind of instrument and ionization; some may be due to inhomogeneous material being released from the nucleus and also the relative location of the two instruments on the lander.

Table 3. Parent molecules detected in the ROSINA–DFMS mass spectra in the mass range 13–62 Da.

Molecule		Mass
CH_4	Methane	16
NH_3	Ammonia	17
H_2O	Water	18
CHN	Hydrogen cyanide	27
CO	Carbon monoxide	28
C_2H_6	Ethane	30
CH_2O	Formaldehyde	30
CH_5N	Methylamine	31
CH_4O	Methanol	32
CH_3CN	Acetonitrile (?)	41
CHNO	Isocyanic acid	43
CO_2	Carbon dioxide	44
C_2H_4O	Acetaldehyde	44
C_3H_8	Propane	44
CH_3NO	Formamide	45
C_2H_6O	Ethanol	46
CH_2S	Thioformaldehyde	46
CH_2O_2	Formic acid	46
CH_2S	Methanethiol	48
C_4H_{10}	Butane	58
C_2H_6O	Acetone	58
CH_3CONH_2	Acetamide	59
C_3H_9N	Propylamine	59
C_3H_8O	Propanol	60
$C_2H_4O_2$	Acetic acid	60
C_2H_6S	Ethanethiol / Dimethylsulphide	62
$CH_2(OH)CH_2(OH)$	Ethylene glycol	62

3 CONCLUSIONS

During 2014 November 12, Ptolemy and COSAC on board *Philae* measured material from the Agilkia landing site, revealing mostly organic CHO-bearing molecules. During a 'dust event', dust and ice hitting the *Rosetta* spacecraft on 2016 September 5, ROSINA–DFMS measured mass spectra of sublimating gases from solid material in its ionization box in addition to the ambient coma between masses 13 and 100 Da, revealing also a dominance of CHO-bearing molecules. While absolute and relative abundances differ between the three instruments, the results on the organics are qualitatively compatible. Hydrocarbons are abundant as seen in the DFMS mass spectra. CHN- and CHS-bearing molecules have similar abundances, depleted by about a factor of 3 compared to CH-bearing, whereas CHO_2- and CHNO-bearing molecules are depleted by about a factor of 10. In the mass range 12–62 Da, at least 25 organic molecules contribute to the signal observed in DFMS (see Table 3). In addition, there are some abundant inorganics like O_2, H_2S and SO_2 (SO) together with a few less abundant ones (e.g. N_2) in the spectra of DFMS, but not in the spectra of COSAC or Ptolemy. This can be understood as these molecules are very volatile and may have disappeared from the sample measured on the nucleus surface

Downloaded from https://academic.oup.com/mnras/article/469/Suppl_2/S130/3865958 by guest on 11 November 2020

before ending up in the mass spectrometers, or they may have sublimated in the instruments themselves due to the storage for >20 min at ∼15°C before measurements started. Using the combination of the three data sets, the list of molecules observed from Agilkia must be expanded to include contributions of many more molecules with e.g. S-bearing species as well as higher mass complex organics than suggested by Ptolemy and COSAC. The dominant molecule on mass 44 is most probably CO_2 in all three measurements in particular when considering the position of the mass peak in the COSAC spectrum. Methyl isocyanate, propanal and glycol aldehyde were not confirmed by DFMS measurements and suggest a revision of the list of molecules given in Goesmann et al. (2015) (see Table 1) and especially their derived abundances. The high peaks at masses 91 and 92 Da seen in the Ptolemy spectrum could very well be due to the aromatic molecule toluene (CH_3–C_6H_5). Toluene is regularly seen in DFMS spectra and the fragmentation pattern is compatible with the Ptolemy spectrum.

Overall the results are consistent with the observations made by VIRTS of a mixture of saturated and unsaturated hydrocarbons and OH-bearing molecules with little nitrogeneous material (Capaccioni et al. 2015). However, we do not see a significant amount of semivolatile carboxylic acid as postulated by VIRTIS (Quirico et al. 2016) to explain the broad absorption feature observed. The amount of COOH-bearing molecules is rather small in the mass range considered here. However, we cannot exclude more heavy or more refractory species, which do not or only marginally sublimate at 275 K.

Due to the limited mass resolution and the low counting statistics, the interpretation of the COSAC and Ptolemy spectra is by far not unique. There are probably many solutions that fit the spectra equally well and one has to be very careful to draw too many conclusions. An example of an alternative fit to the COSAC data is given in Appendix B. Only by thoroughly analysing ROSINA–DFMS high-resolution spectra over the whole mass range and after careful calibration of as many fragmentation patterns as possible with the DFMS twin instrument in the laboratory can we deduce quantitative abundances of major and minor species from the complex mass spectra. This will lead to a revision of which species to include/exclude when fitting the lower resolution mass spectra obtained on the surface of 67P by the *Philae* instruments and of the chemical network to be used. However, the initial examination of the combined results of all three instruments already shows a very rich organic inventory of the ice–dust mixture of 67P/Churyumov–Gerasimenko, much richer than previously considered, which will help to unravel the origin of this carbonaceous material.

ACKNOWLEDGEMENTS

The following institutions and agencies supported this work: Univversity of Bern was funded by the State of Bern, the Swiss National Science Foundation and by the European Space Agency PRODEX Program. Work at Southwest Research institute was funded by Jet Propulsion Laboratory (subcontract no. 1496541), at the University of Michigan by NASA (contract JPL-1266313), by CNES grants at Laboratoire Atmosphères, Milieux, Observations Spatiales, and at Royal Belgian Institute for Space Aeronomy by the Belgian Science Policy Office via PRODEX/ROSINA PEA 90020. COSAC was supported by DLR under contract number 50 QP 1302. IW and AM would like to thank the following agencies for financial support and continuing interest in this project: the Science and Technology Facilities Council (Consolidated Grants ST/L000776/1 and ST/P000657/1) and the UK Space Agency (Post-launch support ST/K001973/1); we would also like to acknowledge the efforts of all of the Ptolemy co-investigators. ROSINA would not give such outstanding results without the work of the many engineers, technicians and scientists involved in the mission, in the *Rosetta* spacecraft, and in the ROSINA instrument team over the last 20 yr whose contributions are gratefully acknowledged. *Rosetta* is an ESA mission with contributions from its member states and NASA. We acknowledge herewith the work of the whole ESA *Rosetta* team.

All ROSINA, Ptolemy and COSAC data have been released to the public PSA archive of ESA (https://www.cosmos.esa.int/web/psa/rosetta) and to the PDS archive of NASA.

REFERENCES

Balsiger H. et al., 2007, Space Sci. Rev., 128, 745
Biele J. et al., 2015, Science, 349, aaa9816
Calmonte U. et al., 2016, MNRAS, 462, S253
Capaccioni F. et al., 2015, Science, 347, aaa0628
Cottin H., Bénilan Y., Gazeau M. C., Raulin F., 2004, Icarus, 167, 397
Finzi A. E. et al., 2007, Space Sci. Rev., 128, 281
Fornasier S. et al., 2015, A&A, 583, A30
Fray N. et al., 2016, Nature, 538, 72
Goesmann F. et al., 2007, Space Sci. Rev., 128, 257
Goesmann F. et al., 2015, Science, 349, aab0689
Graf S. et al., 2004, Geophys. Res.: Planets, 109, E7
Grün E. et al., 2016, MNRAS, 462, S220
Hässig M. et al., 2015, Science, 347, aaa0276
Huebner W., 1987, Science, 237, 628
Korth A. et al., 1986, Nature, 321, 335
Krüger H. et al., 2017, A&A, 600, A56
Meier R., Eberhardt P., Krankowsky D., Hodges R. R., 1993, A&A, 277, 677
Mitchell D. L. et al., 1989, Adv. Space Res., 9, 35
Morse A., Morgan G., Andrews D., Barber S., Leese M., Sheridan S., Wright I., Pillinger C., 2009, Ptolemy-a GCMS to Measure the Chemical and Stable Isotopic Composition of a Comet. Springer, Berlin
Morse A., Mousis O., Sheridan S., Morgan G., Andrews D., Barber S., Wright I., 2015, A&A, 583, A42
Nevejans D., Neefs E., Kavadias S., Merken P., Van Hoof C., 2002, Int. J. Mass Spectrom., 215, 77
Quirico E. et al., 2016, Icarus, 272, 32
Rubin M., Tenishev V. M., Combi M. R., Hansen K. C., Gombosi T. I., Altwegg K., Balsiger H., 2011, Icarus, 213, 655
Rubin M. et al., 2015, Science, 348, 232
Stein S. E., 2016, in Linstrom P. J., Mallard W. G., eds, NIST Chemistry WebBook, NIST Standard Reference Database Number 69. National Institute of Standards and Technology, Gaithersburg, MD
Stern S. A. et al., 2015, Icarus, 256, 117
Thomas N. et al., 2015, Science, 347, aaa0440
Ulamec S. et al., 2016, Acta Astronaut., 125, 80
Wright I. P., Sheridan S., Barber S. J., Morgan G. H., Andrews D. J., Morse A. D., 2015, Science, 349, aab0673

Downloaded from https://academic.oup.com/mnras/article/469/Suppl_2/S130/3865958 by guest on 11 November 2020

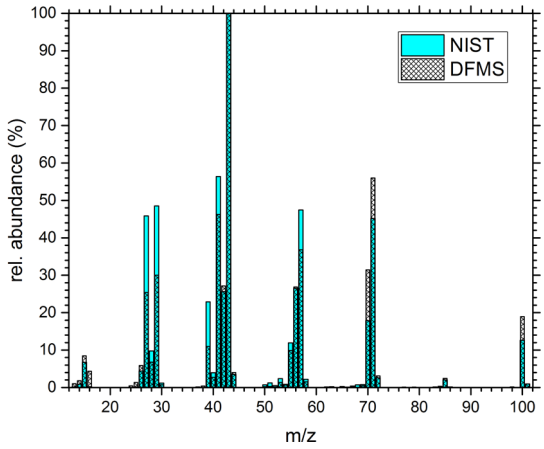


Figure A1. Comparison of NIST and ROSINA–DFMS fragmentation patterns for *n*-heptane.

APPENDIX A: FRAGMENTATION PATTERN COMPARISON

The NIST data base used for this study for fragmentation pattern uses data from electron impact ionization with the electron energy at 70 eV. The same energy is used by all mass spectrometers mentioned in the main text except ROSINA–DFMS. There the electron energy used is 45 eV. Fragmentation patterns depend not only on this energy, but also on the specific characteristics of the mass dispersion elements used in the sensors. We show here a comparison of the NIST-derived fragmentation pattern and calibration data for ROSINA–DFMS in Fig. A1. The patterns are similar, but by no means identical. For this study, which contains only qualitative interpretation, this is sufficient. For a detailed study giving abundances, the parent molecules have to be calibrated in the laboratory using the twin instrument of ROSINA–DFMS.

APPENDIX B: ALTERNATIVE FIT TO THE COSAC DATA

With the unit mass resolution of COSAC and the low count rates there are many solutions to fit the spectra. It is clear that not all of them make sense looking at the chemistry involved. As an example we show here one alternative fit in Fig. B1 with the molecules of Table B1. The fit is clearly better than the original fit; however, the selection of molecules is somewhat arbitrary. But it shows that there are multiple solutions to explain the data of COSAC.

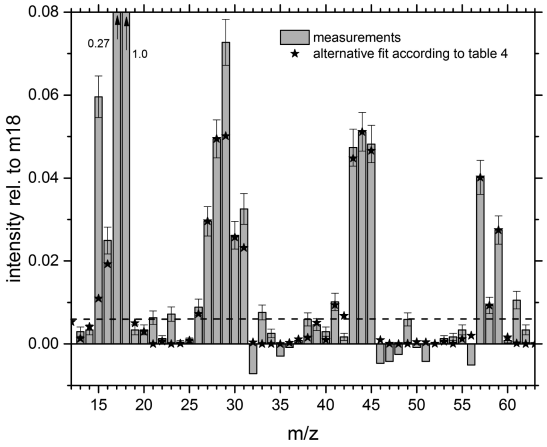


Figure B1. Alternative fit of the COSAC data (Goesmann et al. 2015) with the molecules of Table B1.

Table B1. List of alternative parent molecules used for fitting the COSAC spectrum in Goesmann et al. (2015).

Molecule		Mass	Rel. abundance
H_2O	Water	18	80.0
CHN	Hydrogen cyanide	27	1.3
CO	Carbon monoxide	28	2.2
CH_5N	Methylamine	31	2.0
C_2H_4O	Ethylene oxide	44	0.6
CO_2	Carbon dioxide	44	2.7
C_3H_6O	Acetone	58	2.6
$C_4H_{10}O$	2-Methyl-2-propanol	74	2.2
$C_5H_{10}O$	3 Pentanone	86	2.8

This paper has been typeset from a TEX/LATEX file prepared by the author.

Downloaded from https://academic.oup.com/mnras/article/469/Suppl_2/S130/3865958 by guest on 11 November 2020